elements of the space group $P2_1/n$, contains two formula units of $[(NH_3)_5Os(pyz)Os(NH_3)_5]Cl_6 \cdot 2H_2O$ each residing on crystallographic inversion centers. Table II contains positional parameters and estimated standard deviations for the non-hydrogen atoms, while Tables III and IV contain bond lengths and bond angles, respectively. Also shown in Tables III and IV are the equivalent values in the isostructural ruthenium complex.[5] The molecular structure and numbering system used are given in Figure 1.

The pyrazine ring forms angles of 43.87° with the plane defined by Os, N(2),[11] N(3), N(4), and N(6) and 47.32° with the plane defined by Os, N(1), N(2), N(5), and N(6). The cis-$NH_3$ groups are slightly compressed away from the pyrazine group. The shortest Os-N bond length is observed for the Os-N(pyz) bond. Other variations in the Os-N bonds may be attributed to hydrogen bonding with the water molecules of crystallization and $Cl^-$ counterions.

## Discussion

The Os-$NH_3$ bond lengths of 2.112-2.130 Å in $[(NH_3)_5Os(pyz)Os(NH_3)_5]Cl_6 \cdot 2H_2O$ are similar to those in $[Os(en)_3](CF_3SO_3)_3 \cdot H_2O$,[12] where the average Os-N bond length is 2.11 Å. However, the Os-N(pyz) bond length of 2.101 (7) Å is shorter than the Os-N(ammine) bonds. The shortening of the Os-N(pyz) bond by $\pi$-back-bonding is particularly evident when the isostructural Ru and Os compounds are compared (see Table III). Contrary to the observations for Os, the Ru-N(pyz) bond is the longest bond, and the Ru-N(trans) bond is about the shortest. The ruthenium result is expected when $\pi$-bonding is small, since pyrazine and pyrazinium ions are much poorer $\sigma$-donors than is ammonia. Further, electrostatic repulsion between the metal centers would tend to weaken the M-N(pyz) bonds. The strength of the $\pi$-interaction in the Os(III) complex is demonstrated by both these effects being counteracted. It is expected that the $\pi$-back-bonding interaction be stronger for the osmium complex because the Os(III) valence d orbitals are much closer in energy to the $\pi^*$ ligand orbitals than is the case for Ru(III).

Kinetic, thermodynamic, and spectroscopic data exist to support the structural evidence presented here for significant $\pi$-back-bonding for Os(III). For instance, $[Os(NH_3)_5NCR]^{3+}$ complexes undergo nitrile hydrolysis at rates orders of magnitude lower than the ruthenium analogues.[13] Further, the Os(III) dinitrogen complexes have stabilities toward substitution that are consistent with strong $\pi$-bonding.[14,15] While $[Ru(NH_3)_5CO]^{3+}$ is not known, $[Os(NH_3)_5CO]^{3+}$ does exist[22] and shows a carbonyl stretching frequency of 2058 $cm^{-1}$, significantly lower than that of free carbon monoxide.

In all the known structures[5,13-21] of Os(II), Os(III), Ru(II) and Ru(III) ammine complexes containing N-heterocyclic ligands, the ligand plane bisects the N-M-N angles formed by the cis ligands. The major reason for this is that the staggered conformation minimizes steric clashes between the hydrogen atoms of the heterocycle and those of the cis ammines. The steric effects of nitrogen heterocycles have frequently been noted in pyridine complexes of Co(III), for example *trans*-$[(NH_3)_4pyCoNO_2]Br_2 \cdot H_2O$,[23] *trans*-$Co(DMG)_2(py)CH_2C(CH_3)_3$,[24] and CoTPP-$(OCH_3)py$.[25] The net result of the staggered conformation is that the d$\pi$ set of orbitals includes $d_{xy}$, $d_{yz}$, and $d_{x^2-y^2}$, and the antibonding set consists of the $d_{xy}$ and $d_{z^2}$ orbitals. Due to the low symmetry, the d$\pi$ set is not completely nonbonding with respect to the ligand $\sigma$ orbitals, and splitting between the orbitals of the d$\pi$ set (before consideration of $\pi$ effects) is possible. Without a calculation, the direction of the splitting cannot be predicted, but the magnitude is assuredly small, due to the poor overlap of the orbitals involved.

**Acknowledgment.** P.A.L. is grateful for the receipt of CSIRO and Queen Elizabeth II Fellowships. We are also grateful for support from National Science Foundation Grant No. CHE79-08633 and National Institutes of Health Grant No. GM13638-17 and to Dr. A. Ludi for kindly supplying information on the structures of the ruthenium complexes prior to publication.

**Registry No.** $[(NH_3)_5Os(pyz)Os(NH_3)_5]Cl_6 \cdot 2H_2O$, 98194-39-9.

**Supplementary Material Available:** Listings of structure factor amplitudes (observed and calculated) and thermal parameters (12 pages). Ordering information is given on any current masthead page.

(11) The least-squares plane of the pyrazine ring (plane 1) includes N(6), C(1), and C(2) and is defined by the equation $-4.4347x - 0.75989y - 10.049z + 2.2311 = 0$. The osmium atom is 0.072 Å from the plane. Plane 2 contains Os, N(2), N(3), N(4), and N(6) and is defined by the equation $6.387x + 5.356y + 1.147z - 3.190 = 0$. The atoms for plane 3 are Os, N(1), N(2), N(5), and N(6). Plane 3 is defined by $-0.1504x - 5.069y + 12.933z + 0.1415 = 0$. Angles between planes: 1 and 2, 43.87°; 1 and 3, 47.32°; 2 and 3, 91.11°.

(12) Lay, P. A.; McLaughton, G. M.; Sargeson, A. M., to be submitted for publication.
(13) Lay, P. A.; Magnuson, R. H.; Taube, H., in preparation.
(14) Buhr, J. D.; Taube, H. *Inorg. Chem.* **1980**, *19*, 2425.
(15) Lay, P. A.; Magnuson, R. H.; Taube, H.; Ferguson, J.; Krausz, E. R. *J. Am. Chem. Soc.* **1985**, *107*, 2551-2552.
(16) Sundberg, R. J.; Bryan, R. F.; Taylor, I. F., Jr.; Taube, H. *J. Am. Chem. Soc.* **1974**, *96*, 381.
(17) Krentzien, H. J.; Clarke, M. J.; Taube, H. *Bioinorg. Chem.* **1975**, *4*, 143-151.
(18) Clarke, M. J.; Taube, H. *J. Am. Chem. Soc.* **1975**, *97*, 1397.
(19) Richardson, D. E.; Walker, D. D.; Sutton, J. E.; Hodgson, K. O.; Taube, H. *Inorg. Chem.* **1979**, *18*, 2216.
(20) Wishart, J. F.; Bino, A.; Taube, H., submitted for publication.
(21) Gress, M. E.; Creutz, C.; Quicksall, C. O. *Inorg. Chem.* **1981**, *20*, 1522.
(22) Buhr, J. D.; Taube, H. *Inorg. Chem.* **1979**, *18*, 2208.
(23) Edelmann, F.; Behrens, U. *Z. Anorg. Allg. Chem.* **1977**, *432*, 58.
(24) Randaccio, L.; Bresciani-Pahor, N.; Toscano, P. J.; Marzilli, L. G. *J. Am. Chem. Soc.* **1981**, *103*, 6347.
(25) Riche, C.; Chiaroni, A.; Perree-Fauvet, M.; Gaudemer, A. *Acta Crystallogr., Sect. B: Struct. Crystallogr. Cryst. Chem.* **1978**, *B34*, 1868.

Contribution from the Chemistry Center, Instituto Venezolano de Investigaciones Científicas, Caracas 1010-A, Venezuela, and Istituto Chimico "G. Ciamician" dell'Università, 40126 Bologna, Italy

# Interaction of $H_3Os_4(CO)_{12}I$ with Bis(triphenylphosphine)nitrogen(1+) Nitrite ([PPN][$NO_2$]). Synthesis and Chemical Characterization of [PPN][$H_2Os_4(CO)_{12}I$] and $H_3Os_4(CO)_{11}(NO)$ and X-ray Crystal Structure Determination of the New Nitrosyl Cluster $H_3Os_4(CO)_{11}(NO)$

José Puga,*[1] Roberto Sánchez-Delgado,[1] and Dario Braga*[2]

*Received October 8, 1984*

The reactivity of metal carbonyl clusters is often correlated with the metal core arrangements present in these complexes. Compounds with "open" structures tend to be more reactive than those showing "closed" configurations; we have observed this type of metal framework effect, for instance, in the homogeneous hydrogenation of cyclohexene catalyzed by tetranuclear osmium clusters.[3]

A structural flexibility involving interconversion between "closed" and "open" structures should therefore play an important role in the chemistry and catalytic properties of metal clusters. A number of routes can be envisaged to promote metal core

(1) Instituto Venezolano de Investigaciones Científicas.
(2) Istituto Chimico "G. Ciamician".
(3) Sánchez-Delgado, R. A.; Puga, J.; Rosales, M. *J. Mol. Catal.* **1984**, *24*, 221-225.

0020-1669/85/1324-3971$01.50/0 

rearrangements; thus, electrophilic addition of small molecules to anionic clusters represents a convenient alternative to induce metal–metal bond rupture.[4-6] In contrast, nucleophilic attack on neutral metal clusters has been shown to proceed in some cases with metal–metal bond formation.[7,8]

A different way of enhancing the reactivity of metal carbonyl clusters has been the substitution of one or more CO groups by nitrosyl ligands, which are known to exert an activating influence.[9] However, examples of clusters containing the NO ligand are still relatively scarce. Nucleophilic nitrosylations of $M_3(CO)_{12}$ (M = Ru, Os), $Ru_6C(CO)_{17}$, and $Os_{10}C(CO)_{24}I_2$ have been achieved with $[PPN][NO_2]$ (**1**) in aprotic solvents.[7,8,10,11] This nitrite salt, however, has also been found to act as a deprotonating agent for hydride-containing metal carbonyl clusters.[12,13]

In this paper we report the reaction of the neutral tetranuclear cluster $H_3Os_4(CO)_{12}I$ (**2**) with **1** to form the anionic species $[H_2Os_4(CO)_{12}I]^-$ (**3**) and a new nitrosyl derivative $H_3Os_4(CO)_{11}(NO)$ (**4**) in which a tetrahedral metal configuration is present. The spectroscopic properties of both compounds, as well as the X-ray crystal and molecular structure of the new complex (**4**), are reported.

## Results and Discussion

The tetranuclear iodide cluster $H_3Os_4(CO)_{12}I$ (**2**) reacts with the nitrite ion (as its PPN salt) in dry THF to yield the known compound $[PPN][H_2Os_4(CO)_{12}I]$ (**3**) as the major product. This

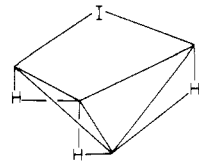


**2**

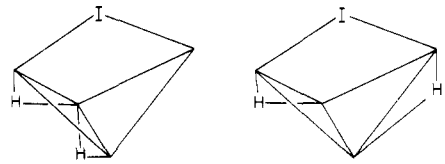


**3a** **3b**

method of preparing **3**, as well as other routes we have investigated (Scheme I), are more convenient than the one previously reported,[13] which involves prolonged reaction of $[H_3Os_4(CO)_{12}(NCMe)_2][BF_4]$ with KI. Although the IR spectrum of **3** has been reported, no NMR data are available. The $^1H$ NMR spectrum in the hydride region with $CD_2Cl_2$ as solvent at 30 °C consists of two broad signals that are resolved at −20 °C into two doublets at −19.74 and −21.66 ppm; $J_{H-H}$ = 1.07 Hz (see Supplementary Figure A). This spectrum differs from that of the parent neutral complex (**2**), in which no H–H coupling is observed.[14] Of the two probable stereochemistries for this compound, only **3a** is consistent with the spectroscopic data, since **3b** should give rise to a singlet corresponding to two equivalent protons. Protonation of this anion with $H_2SO_4$ in $CH_2Cl_2$ regenerates compound **2** almost quantitatively.

A second product of this reaction is the new nitrosyl cluster $H_3Os_4(CO)_{11}(NO)$ (**4**), which was isolated in low yield. The IR spectrum of this compound in $CH_2Cl_2$ solution (Supplementary Figure B) shows a band at 1735 $cm^{-1}$ assigned to the presence of a terminal NO ligand. The $^1H$ NMR spectrum in $CD_2Cl_2$ at

Scheme I[a]

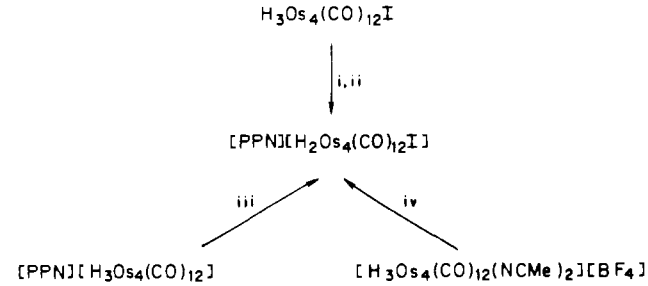


[a] Conditions: (i) $[PPN][NO_2]$, THF, 1 h; (ii) [PPN][I], $CH_2Cl_2$, 3 days; (iii) $I_2$, $CH_2Cl_2$, 3 days; (iv) KI, MeCN, 3 days.[13]

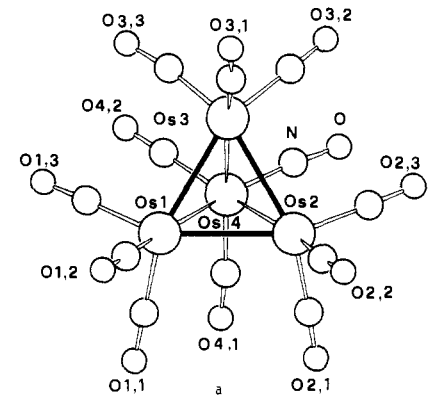


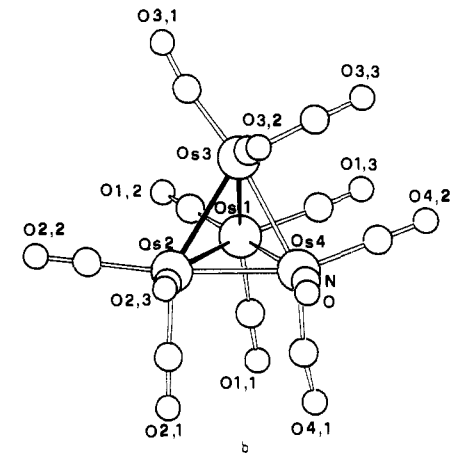


**Figure 1.** Structure of $H_3Os_4(CO)_{11}(NO)$ viewed through the H-bridged (a) and an unbridged (b) triangular face of the tetrahedron, showing the ligand arrangement. Solid bonds are bridged by hydrogen atoms. The tentative NO position is indicated. The C atoms of the CO ligands bear the same labeling as the O atoms.

(4) Farrar, D. H.; Jackson, P. G.; Johnson, B. F. G.; Lewis, J.; Nelson, W. J. H.; Vargas, M. D.; McPartlin, M. *J. Chem. Soc., Chem. Commun.* **1981**, 1009–1011.
(5) Braga, D.; Henrick, K.; Johnson, B. F. G.; Lewis, J.; McPartlin, M.; Nelson, W. J. H.; Puga, J. *J. Chem. Soc., Chem. Commun.* **1982**, 1083–1084.
(6) Braga, D.; Johnson, B. F. G.; Lewis, J.; Mace, J. M.; McPartlin, M.; Puga, J.; Nelson, W. J. H.; Raithby, P. R.; Whitmire, K. H. *J. Chem. Soc. Chem. Commun.* **1982**, 1081–1083.
(7) Johnson, B. F. G.; Lewis, J.; Nelson, W. J. H.; Nicholls, J. N.; Vargas, M. D. *J. Organomet. Chem.* **1983**, *249*, 255–272.
(8) Braga, D.; Johnson, B. F. G.; Lewis, J.; McPartlin, M.; Nelson, W. J. H.; Puga, J.; Vargas, M. D., to be submitted for publication.
(9) Bhaduri, S.; Johnson, B. F. G.; Lewis, J.; Watson, D. J.; Zuccaro, C. *J. Chem. Soc., Dalton Trans.* **1979**, 557–561.
(10) Stevens, R. E.; Yanta, T. J.; Gladfelter, W. L. *J. Am. Chem. Soc.* **1981**, *103*, 4981–4982.
(11) Johnson, B. F. G.; Lewis, J.; Nelson, W. J. H.; Puga, J.; McPartlin, M.; Sironi, A. *J. Organomet. Chem.* **1983**, *253*, C5–C8.
(12) Collins, M. A.; Johnson, B. F. G.; Lewis, J.; Mace, J. M.; Morris, J.; McPartlin, M.; Nelson, W. J. H.; Puga, J.; Raithby, P. R. *J. Chem. Soc., Chem. Commun.* **1983**, 689–691.
(13) Johnson, B. F. G.; Lewis, J.; Nelson, W. J. H.; Puga, J.; Raithby, P. R.; Whitmire, K. H. *J. Chem. Soc., Dalton Trans.* **1983**, 1339–1344.
(14) Johnson, B. F. G.; Lewis, J.; Raithby, P. R.; Sheldrick, G. M.; Wong, K.; McPartlin, M. *J. Chem. Soc., Dalton Trans.* **1978**, 673–676.

**Table I.** Fractional Atomic Coordinates and Thermal Parameters (Å²)

| atom | x | y | z | $U_{iso}$ or $U_{eq}$ |
|---|---|---|---|---|
| Os(1) | −0.0128 (1) | 0.3815 (1) | 0.7818 (1) | 0.035 (1) |
| Os(2) | 0.2040 (1) | 0.0516 (1) | 0.7612 (1) | 0.037 (1) |
| Os(3) | 0.3395 (1) | 0.2580 (1) | 0.8401 (1) | 0.037 (1) |
| Os(4) | 0.2862 (1) | 0.2965 (2) | 0.6388 (1) | 0.048 (1) |
| C(1,1) | −0.1713 (38) | 0.4093 (41) | 0.6898 (21) | 0.056 (8) |
| O(1,1) | −0.2659 (26) | 0.4280 (28) | 0.6322 (15) | 0.061 (6) |
| C(1,2) | −0.1979 (45) | 0.4081 (38) | 0.8922 (25) | 0.051 (8) |
| O(1,2) | −0.3134 (44) | 0.4314 (38) | 0.9570 (25) | 0.050 (6) |
| C(1,3) | −0.0212 (43) | 0.5982 (37) | 0.7555 (23) | 0.045 (7) |
| O(1,3) | −0.0330 (36) | 0.7222 (32) | 0.7452 (20) | 0.069 (7) |
| C(2,1) | 0.1009 (45) | 0.0065 (39) | 0.6606 (26) | 0.053 (8) |
| O(2,1) | 0.0385 (33) | −0.0153 (28) | 0.5992 (18) | 0.064 (7) |
| C(2,2) | 0.1112 (40) | −0.0784 (34) | 0.8642 (22) | 0.040 (6) |
| O(2,2) | 0.0674 (36) | −0.1631 (31) | 0.9236 (20) | 0.070 (7) |
| C(2,3) | 0.4194 (40) | −0.1013 (34) | 0.7163 (22) | 0.042 (7) |
| O(2,3) | 0.5535 (37) | −0.1934 (31) | 0.6914 (20) | 0.072 (7) |
| C(3,1) | 0.3409 (55) | 0.2161 (48) | 0.9814 (8) | 0.074 (11) |
| O(3,1) | 0.3577 (37) | 0.2020 (33) | 1.0654 (8) | 0.079 (8) |
| C(3,2) | 0.5804 (13) | 0.1446 (31) | 0.8056 (21) | 0.043 (7) |
| O(3,2) | 0.7264 (13) | 0.0841 (30) | 0.7792 (19) | 0.075 (7) |
| C(3,3) | 0.3875 (35) | 0.4456 (30) | 0.8201 (19) | 0.032 (6) |
| O(3,3) | 0.3959 (33) | 0.5724 (29) | 0.8078 (18) | 0.062 (6) |
| C(4,1) | 0.1571 (40) | 0.2901 (34) | 0.5395 (22) | 0.043 (6) |
| O(4,1) | 0.0846 (35) | 0.3020 (30) | 0.4718 (20) | 0.066 (7) |
| C(4,2) | 0.3187 (34) | 0.4921 (30) | 0.6074 (19) | 0.031 (5) |
| O(4,2) | 0.3368 (35) | 0.6118 (31) | 0.5901 (20) | 0.067 (7) |
| N | 0.5065 (44) | 0.1683 (38) | 0.5850 (24) | 0.049 (7) |
| O | 0.6409 (43) | 0.0781 (36) | 0.5474 (23) | 0.086 (9) |

**Table II.** Selected Bond Distances (Å) and Angles (deg), with Estimated Standard Deviations in Parentheses

| | | | |
|---|---|---|---|
| Os(1)–Os(2) | 2.933 (2) | Os(4)–C(4,1) | 1.88 (2) |
| Os(1)–Os(3) | 2.932 (2) | Os(4)–C(4,2) | 1.89 (2) |
| Os(1)–Os(4) | 2.796 (2) | Os(4)–N | 1.86 (2) |
| Os(2)–Os(3) | 2.911 (2) | C(1,1)–O(1,1) | 1.15 (1) |
| Os(2)–Os(4) | 2.811 (2) | C(1,2)–O(1,2) | 1.16 (2) |
| Os(3)–Os(4) | 2.789 (2) | C(1,3)–O(1,3) | 1.10 (1) |
| Os(1)–C(1,1) | 1.89 (1) | C(2,1)–O(2,1) | 1.12 (2) |
| Os(1)–C(1,2) | 1.91 (1) | C(2,2)–O(2,2) | 1.14 (3) |
| Os(1)–C(1,3) | 1.94 (2) | C(2,3)–O(2,3) | 1.15 (2) |
| Os(2)–C(2,1) | 1.89 (3) | C(3,1)–O(3,1) | 1.15 (1) |
| Os(2)–C(2,2) | 1.94 (3) | C(3,2)–O(3,2) | 1.15 (1) |
| Os(2)–C(2,3) | 1.89 (2) | C(3,3)–O(3,3) | 1.17 (2) |
| Os(3)–C(3,1) | 1.90 (1) | C(4,1)–O(4,1) | 1.15 (3) |
| Os(3)–C(3,2) | 1.89 (1) | C(4,2)–O(4,2) | 1.15 (2) |
| Os(3)–C(3,3) | 1.87 (1) | N–O | 1.20 (2) |
| Os(1)–C(1,1)–O(1,1) | 178 (2) | Os(3)–C(3,1)–O(3,1) | 170 (2) |
| Os(1)–C(1,2)–O(1,2) | 177 (3) | Os(3)–C(3,2)–O(3,2) | 175 (2) |
| Os(1)–C(1,3)–O(1,3) | 176 (3) | Os(3)–C(3,3)–O(3,3) | 172 (2) |
| Os(2)–C(2,1)–O(2,1) | 178 (3) | Os(4)–C(4,1)–O(4,1) | 171 (3) |
| Os(2)–C(2,2)–O(2,2) | 175 (3) | Os(4)–C(4,2)–O(4,2) | 179 (2) |
| Os(2)–C(2,3)–O(2,3) | 177 (2) | Os(4)–N–O | 174 (2) |

30 °C consists of a sharp singlet at −19.82 ppm attributed to three equivalent hydride ligands (vide infra).

In order to determine the metal atom arrangement and the ligand distribution in **4**, an X-ray single-crystal analysis was undertaken. The molecular structure of **4** is analogous to that of several reported, tetrahedral, 60-electron clusters such as $[H_4M_4(CO)_{12}]$ and $[H_3M_4(CO)_{12}]^-$ (M = Ru, Os).[15,16] Figure 1 shows two different views of the molecular geometry of this complex. Atomic coordinates are reported in Table I and bond distances and selected angles are listed in Table II. The four Os atoms define a tetrahedron of $C_{3v}$ idealized molecular symmetry with three short (mean 2.799 (2) Å) and three long (mean 2.925 (2) Å) metal–metal bonds, the latter belonging to the same triangular face.

Scheme II

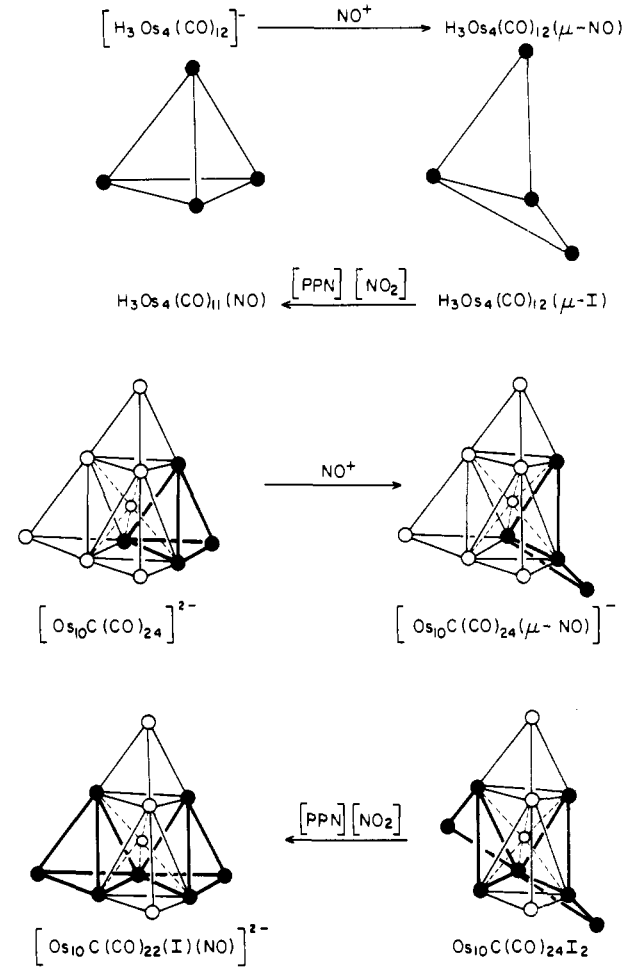


The distribution of the 12 terminal ligands conforms to the idealized symmetry. The ligands pointing away from the triangular face defined by the three long edges appear to be pushed away from the Os–Os bonds (see Figure 1a; Figure 1b shows, for comparison, a view through a different triangular face of the tetrahedron). The presence of three hydrogen atoms bridging the long edges has been inferred on the basis of both metal–metal bond lengthening and CO ligand displacement. Lengthening of Os–Os bonds upon H bridging is a well-established effect, and the structural parameters for bridged and unbridged bonds (2.925 (2) and 2.799 (2) Å, respectively) ought to be compared with the values reported for other derivatives such as $[H_2Os_4(CO)_{12}]^{2-}$[17] (2.934 (4), 2.798 (4) Å), $[H_4Os_4(CO)_{12}]$[15] (2.964 (2), 2.817 (2) Å), and $[H_3Os_4(CO)_{12}]^-$[16] (2.949 (2), 2.798 (2) Å). The metal–hydrogen geometry approximates that of the $C_{3v}$ isomer of the anion $[H_3Ru_4(CO)_{12}]^-$ for which also a $C_2$ solid-state structure is known.[18] Interestingly, only the latter isomer has been identified in the solid state for the analogous anion $[H_3Os_4(CO)_{12}]^-$, although there is some spectroscopic evidence for the presence of two isomers in solution.[14] The Os atom in an apical position with respect to the H-bridged base probably bears the terminal NO ligand (for discussion see the Experimental Section). As a matter of fact the Os–N (1.86 (2) Å) and N–O (1.20 (2) Å) distances are respectively shorter and longer than those of the Os–C and C–O bonds. The average Os–C and C–O distances, 1.90 (2) and 1.14 (2) Å, respectively, are within the range of other reported values for neutral osmium clusters.

(15) Johnson, B. F. G.; Lewis, J.; Raithby, P. R.; Zuccaro, C. *Acta Crystallogr. Sect. B: Struct. Crystallogr. Cryst. Chem.* **1981**, *B37*, 1728–1731.
(16) Johnson, B. F. G.; Lewis, J.; Raithby, P. R.: Zuccaro, C. *Acta Crystallogr. Sect. B: Struct. Crystallogr. Cryst. Chem.* **1978**, *B34*, 3765–3767.
(17) Johnson, B. F. G.; Lewis, J.; Raithby, P. R.; Sheldrick, G. M.; Suss, G. *J. Organomet. Chem.* **1978**, *162*, 179.
(18) Jackson, P. F.; Johnson, B. F. G.; Lewis, J.; McPartlin, M.; Nelson, W. J. H. *J. Chem. Soc., Chem. Commun.* **1978**, 920–921.

**Table III.** Crystal Data and Details of Measurements

| | |
|---|---|
| formula | $H_3C_{11}O_{12}NOs_4$ |
| fw | 1101.9 |
| cryst syst | triclinic |
| $a$, Å | 8.282 (2) |
| $b$, Å | 9.160 (2) |
| $c$, Å | 13.592 (2) |
| $\alpha$, deg | 82.003 (2) |
| $\beta$, deg | 79.850 (2) |
| $\gamma$, deg | 69.016 (2) |
| $V$, Å$^3$ | 939.94 |
| calcd density, g/cm$^3$ | 3.9 |
| $Z$ | 2 |
| space group | $P\bar{1}$, No. 2 |
| $F(000)$ | 946 |
| radiation | graphite-monochromated Mo K$\alpha$ ($\lambda$ = 0.710 69 Å) |
| diffractometer | Nonius CAD4 |
| cryst shape, color | tabular, dark orange |
| cryst size, mm | 0.1 × 0.15 × 0.008 |
| $\mu$(Mo K$\alpha$), cm$^{-1}$ | 259.9 |
| scan range, deg | $2.5 < \theta < 28$ |
| scan type | $\omega/2\theta$ |
| scan interval, deg | 0.7 + 0.35 tan $\theta$ |
| prescan speed, deg min$^{-1}$ | 10 |
| prescan acceptance $\sigma(I)/I$ | 0.5 |
| required final $\sigma(I)/I$ | 0.01 |
| max time, s | 100 |
| bkgd measmt | equal to peak scanning time |
| collcd octants | $\pm h, \pm k, +l$ |
| no. of data collcd at room temp | 3911 |
| no. of data with $I > 3\sigma(I)$ | 2704 |
| equiv reflcns merging | 0.08 |
| no. of azimuthal reflcns used for abs cor | 134 |
| min transmissn, % | 23 |
| max transmissin, % | 98 |
| av cor factor | 0.69 |
| $R$ | 0.0713 |
| $R_w$[a] | 0.0763 |

[a] $R_w = \sum|(F_o - F_c)w^{1/2}|/\sum(F_o w^{1/2})$, where $w$ is equal to $K|\sigma^2(F) + |g|F^2|$; $k$ and $g$ refined to 1.47 and 0.000 52, respectively.

The formation of the two species **3** and **4** from the reaction of **1** with **2** indicates the dual behavior of the $NO_2^-$ ion as both a deprotonating and nucleophilic nitrosylating reagent. The anion (**3**) is expected to possess a butterfly arrangement of metal atoms, analogous to that of the parent compound (**2**), since deprotonation reactions do not usually lead to skeletal rearrangement and since **2** is regenerated by protonation of **3**.

However, closing-up of the metal framework to form the tetrahedral skeleton present in $H_3Os_4(CO)_{11}(NO)$ occurs as a consequence of the nucleophilic attack of the $NO_2^-$ ion.

This type of structural transformation seems to be part of an interesting, and perhaps general, reactivity pattern of metal clusters. Thus, *electrophilic* addition of $NO^+$ to e.g. $[H_3Os_4(CO)_{12}]^-$ and $[Os_{10}C(CO)_{24}]^{2-}$ yields the nitrosyl-*bridged* derivatives $H_3Os_4(CO)_{12}(\mu\text{-}NO)$[6] and $[Os_{10}C(CO)_{24}(\mu\text{-}NO)]^-$,[5] respectively; in both cases the conversion of a tetrahedral arrangement of metal atoms into a butterfly structure *via metal–metal bond scission* is involved (Scheme II).

Conversely, *nucleophilic* attack of $NO_2^-$ to $H_3Os_4(CO)_{12}I$ as herein reported, as well as to $Os_{10}C(CO)_{24}I_2$,[7,8] yields compounds with *terminally bound nitrosyl ligands*, viz. $H_3Os_4(CO)_{11}(NO)$ and $[Os_{10}C(CO)_{22}(NO)I]^{2-}$; in these instances, conversion of a butterfly arrangement of metal atoms into a tetrahedral structure *via metal–metal bond formation* (Scheme II) is involved.

We are currently investigating the reactions of other metal clusters with electrophilic and nucleophilic nitrosylating agents in order to test the general validity of these reactivity trends.

## Experimental Section

**General Procedures.** All reactions were carried out under an atmosphere of nitrogen, and the solvents were distilled over appropriate drying agents. Infrared spectra were recorded on a Perkin-Elmer 337 spectrophotometer, and $^1$H NMR spectra were recorded on a Bruker WP-60 spectrometer.

**Preparation of [PPN][$H_2Os_4(CO)_{12}I$] and $H_3Os_4(CO)_{11}(NO)$.** $H_3Os_4(CO)_{12}I$ (100 mg, 0.082 mmol) was dissolved in 100 mL of THF, and solid [PPN][$NO_2$] (55 mg, 0.094 mmol) was added. The solution was stirred for ca. 1 h and the volume reduced under vacuum. Thin-layer chromatography using a 1:1 $CH_2Cl_2$–hexane mixture gave two bands. The first band was extracted with $CH_2Cl_2$, and dark red crystals of $H_3Os_4(CO)_{11}(NO)$ were obtained upon crystallization at −20 °C; yield 5% (4.5 mg, 0.0041 mmol). IR (cm$^{-1}$): $\nu_{CO}$ 2125 (w), 2085 (s), 2035 (s), 2015 (sh); $\nu_{NO}$ 1735 (m). The second band was extracted with $CH_2Cl_2$, obtained as an oil after evaporation of the solvent (yield 60% (86 mg, 0.049 mmol)), and identified as [PPN][$H_2Os_4(CO)_{12}I$]. IR (cm$^{-1}$): $\nu_{CO}$ 2080 (m), 2048 (s), 2018 (s), 1990 (sh).

**Protonation of [PPN][$H_2Os_4(CO)_{12}I$].** [PPN][$H_2Os_4(CO)_{12}I$] (20 mg, 0.011 mmol) was dissolved in 50 mL of $CH_2Cl_2$; $H_2SO_4$ from a dilute mixture of concentrated sulfuric acid in $CH_2Cl_2$ was added. Thin-layer chromatography using a 1:9 $CH_2Cl_2$–hexane mixture as eluent gave $H_3Os_4(CO)_{12}I$ in 80% yield (11 mg, 0.009 mmol).

**Determination of the Structure of $H_3Os_4(CO)_{11}(NO)$.** Crystal data and details of measurements are contained in Table III. For all computations the SHELX[19] package of crystallographic programs was used. The metal tetrahedron was located by direct methods, all light atoms by subsequent difference Fourier synthesis. The Os atoms were allowed to vibrate anisotropically; all light atoms, isotropically.

The space group choice was confirmed by successful refinement. Although direct location of a NO group among several CO groups is often very difficult, a tentative attribution could be trusted in the present case. The N atom of the NO group was recognized among the C atoms by carefully inspecting the thermal parameters after a preliminary refinement of the structure model with all ligands treated as CO's. The soundness of the NO location was strengthened by comparing its bond parameters with those of the CO groups, as described above. Nonetheless, the differences being almost within the range of experimental errors, the occurrence of disorder between the two kinds of ligands cannot be confidently excluded.

An empirical absorption correction was applied. A final difference-Fourier synthesis showed residual peaks lower than 2 e/Å$^3$ in the vicinity of metal atoms.

**Acknowledgment.** We gratefully acknowledge CONICIT for financial support.

**Registry No.** **1**, 65300-05-2; **2**, 67966-16-9; **3**, 98331-78-3; **4**, 98331-79-4.

**Supplementary Material Available:** Figures A and B containing the $^1$H NMR spectrum of **3** and the IR spectrum of **4**, respectively, and listings of anisotropic thermal parameters, additional interatomic angles, and observed and calculated structure factors (18 pages). Ordering information is given on any current masthead page.

(19) (a) SHELX 76 system of computer programs, by G. M. Sheldrick, University of Cambridge, 1976. (b) Atomic scattering factors and anomalous dispersion terms: "International Tables for X-ray Crystallography"; Kynoch Press: Birmingham, England, 1975; Vol. IV, pp 99, 149.